Environment Model Adaptation for Autonomous Exploration

Erik Arthur Nelson

April 23, 2015

The Robotics Institute
School of Computer Science
Carnegie Mellon University
Pittsburgh, Pennsylvania

Thesis Committee:
Nathan Michael, *Chair*
Artur Dubrawski
Vishnu Desaraju

Submitted in partial fulfillment of the requirements for the degree of Master of Science in Robotics.

Abstract

Acknowledgements

Contents

1 Introduction **1**

1.1 Previous Work 3

1.1.1 Geometric Exploration Strategies 4

1.1.2 Information-Theoretic Exploration Strategies 5

1.2 Thesis Problem 8

1.3 Thesis Statement 8

1.4 Outline 9

2 Foundations **10**

2.1 Occupancy Grid Mapping 11

2.2 Active Perception 12

2.3 Action Generation 14

2.3.1 Frontier Seeding 14

2.3.2 Forward-Arc Motion Primitives 15

2.3.3 Lattice Graph Motion Primitives 17

2.4 Generalized Entropies and Divergences 17

2.5 Cauchy-Schwarz Quadratic Mutual Information 21

2.6 Summary of Foundations 22

3 Information-Theoretic Map Compression **24**

3.1 The Principle of Relevant Information . . . 26

3.2 Framing Map Compression as an Optimization . . . 29

3.3 Solving the Optimization . . . 30

3.4 Occupancy Grid Pyramids . . . 31

3.5 Results . . . 31

3.6 Chapter Summary . . . 31

4 **33**

4.1 The Information Bottleneck Method . . . 33

4.2 Optimizing Map Resolution for Sensing . . . 34

4.3 Results . . . 36

4.4 Chapter Summary . . . 36

5 **37**

5.1 Results . . . 37

5.2 Chapter Summary . . . 37

6 Summary, Contributions, and Future Work **38**

6.1 Thesis Summary . . . 38

6.2 Contributions . . . 38

6.3 Future Work . . . 38

6.4 Conclusions . . . 38

Bibliography **39**

List of Tables

3.1 Contingency table for a compression from the OG region m^R to $\tilde{m}^R$. `O` and `E` stand for `OCC` and `EMP`. 32

List of Figures

1.1 A household service robot awakes in an unknown environment. Prior to accomplishing its main functionalities, it will require a map of its surroundings. What sequence of actions should it take to minimize the time it spends exploring? 2

1.2 A partially explored map with frontiers between free and unknown space highlighted in blue. 4

1.3 Traditional frontier exploration would visit the green location first because it is closest. A simple extension involves simulating sensor measurements from frontiers and examining their informativeness [12]. Applying this extension would cause robot to visit the red frontier first, since that location will provide more information about the map per unit time. 6

1.4 Two variants of mutual information (Fig. 1.4b: Shannon; Fig. 1.4c: Cauchy-Schwarz Quadratic) densely computed in free space over an occupancy grid (Fig. 1.4a) using a 100-beam omnidirectional 2D laser with 30 m range. An exemplary sensor measurement is depicted in Fig. 1.4a. Controlling the robot towards locations that maximize either variant of mutual information would attract the robot to locations from which it could observe unknown areas of the map. 7

2.1 Nine motion primitives generated with $\omega = \{-0.05, -0.04, \ldots, 0.05\}$ rad/s, $v = 1.0$ m/s. 15
2.2 A primitive dictionary with a depth of three constructed from a library of four motion primitives. 16
2.3 An $11 \times 11 \times 1$ lattice graph generated by solving a BVP from the robot's initial pose (middle, facing right) to a lattice of final poses (with final angle equal to initial angle) subject to linear and angular velocity constraints. No solution exists for the nodes immediately above and below the robot's initial position. 18

3.1 Time (median of 10^5 samples) to evaluate CSQMI for a single beam is linear in both the OG resolution Δ, and the measurement range. . . 25
3.2 For each square (cubic in 3D) region m^R in the uncompressed OG m^K, the PRI optimization finds a random variable $\tilde{m}^R$ that minimizes (3.1) and is constrained to have uniform occupancy probability $\tilde{o}^R = (\tilde{o}^1, \ldots, \tilde{o}^1)$. 28

4.1 4.1a shows an uncompressed map and measurement taken from a planned future position. With this map and expected laser scan, the optimal compression level (filled markers) computed with (4.2) decreases as β increases, favoring preservation of information about the measurement as opposed to compression (4.1b). 35

Chapter 1

Introduction

Robots are emerging from controlled factories and laboratories into our homes, workplaces, roads, and public airspaces. Alongside their transition into these unstructured and transient environments comes their need to be able to explore, characterize, and catalog their surroundings. Mobile robot autonomy is generally accomplished by referring to a map - a 2D or 3D probabilistic representation of the locations of obstacles in the robot's workspace. With access to a map, robots can localize to determine their position, plan collision-free trajectories to goals, locate objects for interaction, and make decisions by reasoning about the geometry and dynamics of the world. Given that a robot's map is of critical importance for most autonomy tasks, robots that find themselves initialized without a priori access to a map should be capable of autonomously, efficiently, and intelligently creating one.

The exercise of choosing and executing actions that lead a robot to learn more about its own map is known as *active perception* or *exploration*, and is the central topic of this thesis. Active perception has previously been studied with a multitude of sensor models, environment representations, and robot dynamics models. The active perception task itself can be dissected into two components [33]:

Figure 1.1: A household service robot awakes in an unknown environment. Prior to accomplishing its main functionalities, it will require a map of its surroundings. What sequence of actions should it take to minimize the time it spends exploring?

component 1: Identifying regions in the environment that, when visited, will spatially extend or reduce uncertainty in the current map

component 2: Autonomously navigating to the aforementioned regions, while simultaneously localizing to the map and updating it with acquired sensor measurements

A motivating example is depicted in Fig. 1.1, where a household service robot is initialized in an unknown environment. Prior to accomplishing tasks that a human might ask it to perform, the robot must learn its surroundings and build a map of the house. Ideally this phase of initialization would be fast, as it is a prerequisite to the main functionality of the robot, and also might be required when furniture is moved or household objects are displaced. Where should the robot travel to observe the most of the environment in the shortest amount of time? Virtually any autonomous robot operating in an unknown environment will require a map-building initialization phase, welcoming strategies that enable high-speed and intelligent exploration.

This thesis specifically considers the effects of environment representation on autonomous exploration behaviors, and introduces novel extensions to the active perception task that adaptively modify the environment representation in response to the robot's incoming sensor measurements and current map. The interplay between the robot's environment representation and exploration behaviors is investigated. First, a theory of information-theoretic map compression is developed. The map compression formulation is exercised to examine the information lost about a sensor measurement when compressing a map. Optimizing sensor information loss against map compression allows the robot to choose a resolution with which to represent its environment that maximizes the efficiency of exploration. The information lost through map compression can also be used to analyze the complexity and obstacle density of an environment. This second loss metric is added to the exploration reward function, allowing an autonomously exploring robot to choose trajectories that are both informative and safe for high-speed navigation.

The proposed active perception extensions enable two new capabilities:

1. Compressing the robot's map, when possible, increases the efficiency of computing information-theoretic reward by orders of magnitude, thereby enabling faster planning and navigation during exploration

2. Analyzing the loss in informativeness of sensor measurements when compressing the map enables the robot to choose trajectories are both safe (avoiding obstacle-dense regions) and informative (maximizing an information-based reward).

1.1 Previous Work

Prior approaches to mobile robot active perception fall into two broad categories: *geometric* approaches that reason about the locations and presence of obstacles and free

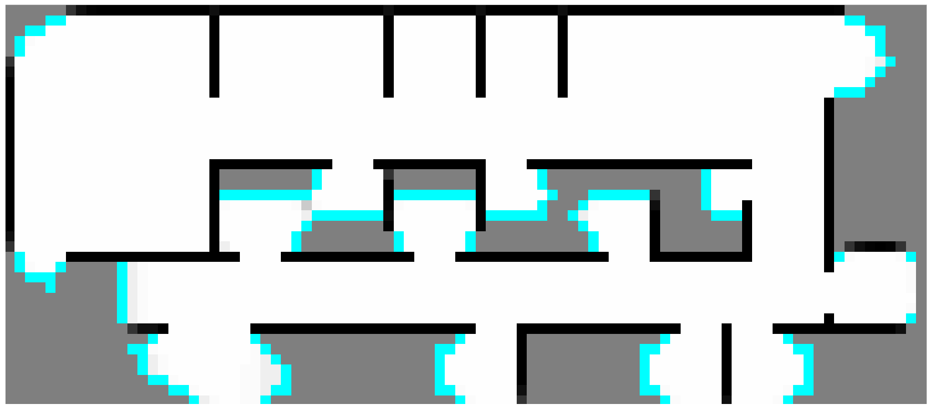

Figure 1.2: A partially explored map with frontiers between free and unknown space highlighted in blue.

space in the robot's map [1, 7, 8, 35, 38, 40], and *information-theoretic* approaches that treat the map as a multivariate random variable and choose actions that will maximally reduce its uncertainty [2, 6, 9, 11, 16]. Both categories of approaches solve **component 1** of active perception, and assume that a planner and Simultaneous Localization and Mapping (SLAM) framework are available to accomplish **component 2**.

1.1.1 Geometric Exploration Strategies

Many successful geometric exploration approaches build upon the seminal work of Yamauchi [40], guiding the robot to *frontiers* - regions on the boundary between free and unexplored space in the map (Fig. 1.2). Since multiple frontiers often exist simultaneously in a partially explored map, a variety of heuristics and spatial metrics can be used to decide which frontier to travel towards [23]. For example, an agent may decide to visit the frontier whose path through the configuration space from the agent's current position has minimum length, or requires minimal time or energy input to traverse. Similarly, an agent may decide to only plan paths to locations from which frontiers can be observed by its onboard sensors.

While effective in 2D environments, frontier exploration algorithms have several restrictive qualities. First, the naïve extension of frontier exploration from 2D to 3D maps poses a non-trivial challenge; as the dimensionality of the workspace increases, frontiers are distributed more densely throughout the environment due to occlusions, sensing resolution, and field-of-view, resulting in poor exploration performance [33]. Second, planning a path to a frontier does not imply that the path itself will be information-rich. Trajectory optimization techniques that consider information acquired by the robot's sensors along a planned path can be used as extensions to improve exploration performance [19, 34]. Finally, although the robot is guaranteed to learn new information upon reaching a frontier, the amount of information learned is dependent on the robot's sensor model, which is not considered when identifying frontiers. It may therefore be more efficient to visit a frontier that is suboptimal according to heuristics such as path length if the robot's sensors will provide more information from that location (Fig. 1.3). This limitation was first overcome by evaluating the informativeness of simulated sensor measurements taken from frontier locations [12], and was the original motivation for developing a category of information-theoretic exploration strategies.

More thorough surveys of frontier exploration algorithms and heuristics are provided by Basilico et al. [5] and Holz et al. [14].

1.1.2 Information-Theoretic Exploration Strategies

Information-theoretic exploration strategies cast the active perception task as an optimization, and choose actions for the robot that maximize an information-based objective function such as Shannon's entropy or mutual information [6, 9, 16, 18] (Fig. 1.4).

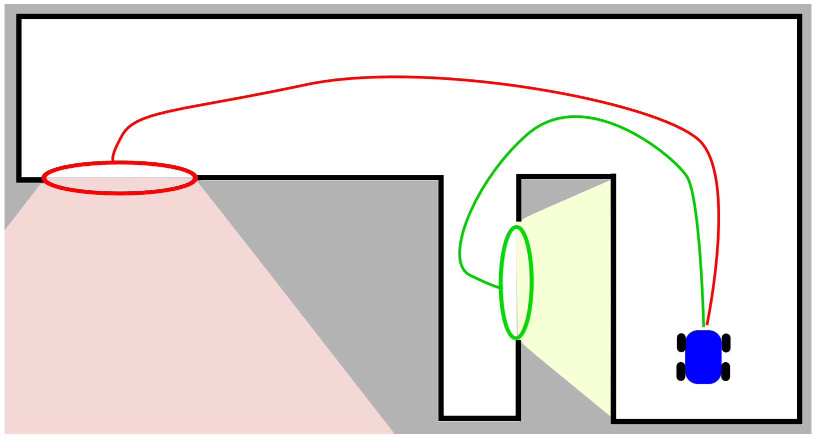

Figure 1.3: Traditional frontier exploration would visit the green location first because it is closest. A simple extension involves simulating sensor measurements from frontiers and examining their informativeness [12]. Applying this extension would cause robot to visit the red frontier first, since that location will provide more information about the map per unit time.

Entropic measures like these are appealing because unlike geometric methods, they capture the relationship between sensor placement and uncertainty in the map. In addition, they can be computed without a maximum likelihood map estimate, and therefore do not discard probabilistic information known to the robot. Control policies that maximize mutual information have been proven to guide robots towards unexplored space [16], and weighting frontiers by the expected mutual information between the map and a sensor measurement acquired at the frontier location has been shown to result in more efficient exploration behaviors than traditional frontier exploration [9]. The exact same calculation can be used to evaluate information-theoretic objective functions in 2D and 3D environments.

The utility afforded by information-theoretic approaches comes at the cost of computational inefficiency. As a point of comparison, frontiers and other geometrically-defined landmarks need only to be computed once per map update, and can be computed (at worst, using a brute force search) with time complexity linear in the

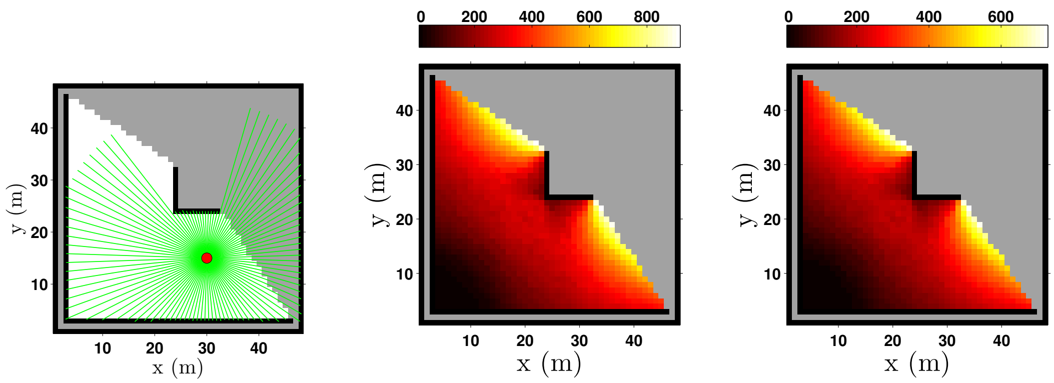

(a) (b) (c)

Figure 1.4: Two variants of mutual information (Fig. 1.4b: Shannon; Fig. 1.4c: Cauchy-Schwarz Quadratic) densely computed in free space over an occupancy grid (Fig. 1.4a) using a 100-beam omnidirectional 2D laser with 30 m range. An exemplary sensor measurement is depicted in Fig. 1.4a. Controlling the robot towards locations that maximize either variant of mutual information would attract the robot to locations from which it could observe unknown areas of the map.

number of cells in the robot's map. One may alternatively choose to identify and cache frontiers every time a sensor measurement is used to update the map, yielding a constant time frontier identification step that is bounded by the number of map voxels within the maximum sensor range. By contrast, information-theoretic objective functions typically consider the probabilistic uncertainty associated with the sensor and environment models, and therefore require expensive sensor-related operations such as raycasts or sampling a large number of times from the distribution of possible future measurements. Approximations to mutual information between a map and beam-based sensor measurements can be evaluated with time complexity linear in the number of map voxels intersected by a sensor's beams [9, 17, 24]. This already-expensive operation must be performed for every future location that the robot might wish to travel to. Julian et al. report that densely calculating mutual information over the free space in a large 1500 m^2 map requires approximately ten seconds with a parallelized implementation using a 3.4 Ghz quad-core CPU and NVIDIA GTX 690 graphics card [16].

1.2 Thesis Problem

Although inefficient, information-theoretic solutions to the active perception task are superior to geometric solutions in many ways. However, modern computers cannot densely evaluate information-theoretic objective functions over a robot's map in real-time. Any strategy that makes the evaluation of information-theoretic objective functions more efficient will allow a robot to consider more future locations prior to taking an action towards one, thereby increasing the speed at which the robot is able to explore an environment.

Currently, the most efficient information-theoretic exploration algorithms are too slow for the motivating scenario described in Fig. 1.1. For example, a highly-efficient recent approach by Charrow et al., requires eleven minutes to explore a 17 m $\times$18 m $\times$3 m building with a quadrotor - enough time for the quadrotor's batteries to deplete twice [9]. This thesis addresses the inefficiencies of information-theoretic exploration, summarized in the following statement:

Thesis Problem: Solutions to the mobile robot active perception task that involve optimization of information-theoretic cost functions are too computationally expensive for high-speed exploration in complex environments.

1.3 Thesis Statement

This thesis proposes occupancy grid compression as a solution to the computational inefficiencies of information-theoretic exploration.

1.4 Outline

Chapter 2

Foundations

This thesis draws upon prior research from the robotics, information theory, and signal processing domains to develop its formulations. Sections 2.1 - 2.3 review relevant topics within robotics including occupancy grid mapping, active perception as an optimization, and several planning strategies that are suitable for the exploration task. These foundational topics will be used to develop a theory of optimal occupancy grid compression as well as methods for guiding a robot to explore uncertain areas of its map efficiently. The formulations developed in Chapters 3 - 5 will also borrow heavily from information theory and rate distortion theory. These domains are frequently concerned with evaluating the effect one random variable (e.g. a sensor measurement) has on another (e.g. a map) or with compressing a random variable to a reduced representation in such a way that the compressed form preserves the structure of the uncompressed form. Sections 2.4 and 2.5 review concepts from these domains that will be used when developing theories for optimal map resolution selection, and for adapting robot exploration behaviors to the resolution with which its environment is modeled.

2.1 Occupancy Grid Mapping

Occupancy grids (OGs) are a common and useful proabilistic map model for representing and reasoning about an unknown environment. The remainder of this thesis assumes that the robot's environment is represented as an OG. Figures 1.2, 1.3 and 1.4a depict occupancy grids, where black cells represent areas of the environment occupied by an obstacle, white cells represent areas that do not contain obstacles, and grey cells represent locations with unknown occupancy status.

OGs decompose the robot's workspace into a discrete set of 2D or 3D cells with a specified resolution. The presence or absence of obstacles within these cells is modeled as a K-tuple binary random variable, $\mathbf{m} = \{m_i\}_{i=1}^{K}$, with support set $\{\texttt{EMP}, \texttt{OCC}\}$. The probability that an individual cell is occupied is given by $p\left(m_i \mid \mathbf{x}_{1:t}, \mathbf{z}_{1:t}\right)$, where $\mathbf{x}_{1:t}$ denotes the robot's history of states, and $\mathbf{z}_{1:t}$ denotes the history of range observations accumulated by the robot. The OG representation treats cells as independent from one another, allowing one to express the probability of a specific map as the product of individual cell occupancy values:

$$p\left(\mathbf{m} \mid \mathbf{x}_{1:t}, \mathbf{z}_{1:t}\right) = \prod_i p\left(m_i \mid \mathbf{x}_{1:t}, \mathbf{z}_{1:t}\right). \tag{2.1}$$

For notational simplicity, the map conditioned on random variables $\mathbf{x}_{1:t}$ and $\mathbf{z}_{1:t}$ will henceforth be written as $p\left(\mathbf{m}\right) \equiv p\left(\mathbf{m} \mid \mathbf{x}_{1:t}, \mathbf{z}_{1:t}\right)$, and the probability of occupancy for a grid cell i as $o_i \equiv p\left(m_i = \texttt{OCC} \mid \mathbf{x}_{1:t}, \mathbf{z}_{1:t}\right)$. Unobserved grid cells are assigned a uniform prior such that $\{o_i = 1 - o_i = 0.5\}_{i=1}^{K}$. This implies that the robot is initially unaware of its surroundings prior to accumulating sensor measurements. To prevent numerical precision issues, the occupancy status of a grid cell m_i is represented by the log-odds ratio

$$l \equiv \log \frac{o_i}{1 - o_i}. \tag{2.2}$$

The log-odds ratio maps from occupancy probabilities existing on $[0, 1]$ to $\mathbb{R}$, which is more suitable for floating-point arithmetic. In addition, the log-odds ratio makes updates to a cell occupancy probability additive rather than multaplicative. When a new measurement $\mathbf{z}_t$ is obtained, cell occupancy values may be updated with

$$l \leftarrow l + L\left(m_i \left| \mathbf{z}_t\right.\right), \tag{2.3}$$

where the term $L\left(m_i \left| \mathbf{z}_t\right.\right)$ represents the robot's inverse sensor model [36].

2.2 Active Perception

Active perception is the idea that a machine should continually guide itself to states in which it is able to acquire better sensor measurements [3, 4]. Active perception draws inspiration from biological sensors that adapt in response to external stimuli. The human eye, for example, has muscles that constrict the pupil in response to bright light (adaptation), and others that distort the curvature of its lens to focus on nearby or far-away objects (accomodation). Adaptation and accomodation allow humans to see light varying nine orders of magnitude in brightness, and focus on objects an infinite distance away. Similarly, a man-made sensor such as a camera should not passively collect and report incoming photons, but should adapt its aperture, CMOS gains, and shutter speed based on the properties of the incoming light.

To extend this idea to mobile robotics, one must consider the robot system itself as a sensor that is able to move and actuate for the purpose of collecting better sensor measurements. From this perspective, the robot's task is to choose and execute *actions* that optimize the quality of its sensor measurements. An action can be defined as a sequence of configurations $\mathbf{x}_\tau \equiv (\mathbf{x}_{t+1}, \ldots, \mathbf{x}_{t+T})$ that the robot will achieve over a future time interval $\tau \equiv (t+1, \ldots, t+T)$. From configurations $\mathbf{x}_\tau$ the robot will acquire future sensor measurements $\mathbf{z}_\tau \equiv (\mathbf{z}_{t+1}(\mathbf{x}_{t+1}), \ldots, \mathbf{z}_{t+T}(\mathbf{x}_{t+T}))$. This thesis is concerned primarily with ground robots constrained to $SE(2)$, and will therefore use $\mathbf{x}_i$ to refer to a pose in 2D space: $\mathbf{x}_i \equiv (x_i, y_i, \theta_i)^T$.

In the context of exploring an unknown environment, the active perception problem can be framed as an optimization over possible future actions that the robot can take:

$$\mathbf{x}_\tau^* = \underset{\mathbf{x}_\tau \in \mathcal{X}}{\operatorname{argmax}} \ \mathcal{J}\left(\mathbf{m}, \mathbf{z}_\tau(\mathbf{x}_\tau)\right), \tag{2.4}$$

where $\mathcal{J}\left(\mathbf{m}, \mathbf{z}_\tau(\mathbf{x}_\tau)\right)$ is a reward function expressing the new information learned by sequentially moving the robot to configurations $\mathbf{x}_\tau$, collecting sensor measurements $\mathbf{z}_\tau$, and updating the map $\mathbf{m}$. $\mathcal{X}$ is the set of all collision-free and dynamically feasible actions that the robot can take. In addition to evaluating the pure information content of $\mathbf{z}_\tau$, $\mathcal{J}$ commonly incorporates the length of time or energy expenditure required to carry out the action $\mathbf{x}_\tau$.

Unfortunately, the active perception optimizaton faces the *curse of dimensionality*; the size of $\mathcal{X}$ grows exponentially with the length of the time horizon τ. As τ increases in size, it quickly becomes infeasible to evaluate $\mathcal{J}$ over all possible actions in $\mathcal{X}$. This inefficiency motivates generating a fixed-size set candidate actions that are likely to be informative prior to optimizing (2.4).

2.3 Action Generation

The primary concern of action generation is to suggest a fixed-size set of feasible actions $\mathcal{X}$ that are likely to be informative. A suitable choice of $\mathcal{J}$ can be evaluated on these actions to choose an optimal exploration action using (2.4). Several action generation options exist.

2.3.1 Frontier Seeding

Recent works by Charrow et al. [9] and Vallvé et al. [37] suggest seeding information-theoretic exploration by identifying frontiers and then evaluating a reward function from frontier locations. Because frontier identification is efficient, this two-pass approach is useful for locating potentially informative locations prior to performing the comparatively more expensive reward evaluation step. This strategy has the added benefit that frontiers are computed globally across the robot's map, guaranteeing that the robot will never become trapped in a dead-end or a location where its local map is already fully explored.

Identifying frontiers before planning to them avoids planning feasible trajectories to many future locations. Frontiers can be ranked by the information-theoretic reward offered from their locations, and the resulting sorted list of frontiers can be iterated through until a dynamically feasible and collision-free trajectory is found. Planning from an initial state to a goal state subject to dynamic and obstacle constraints becomes especially expensive in high-dimensional configuration spaces, and should be performed as few times as possible.

After selecting a location that will yield high reward, one may use a real-time pathfinding algorithm such as A* [13], RRT [22], or their many variants to generate a trajectory from the robot's initial state.

2.3.2 Forward-Arc Motion Primitives

Actions can also be generated by sampling from a set of pre-computed motion primitives. A simple strategy for generating motion primitives for a ground vehicle constrained to $SE(2)$ involves simulating the robot's path when moving at a constant linear and angular velocity for a specified amount of time. Actions resulting from this approach form arcs of a circle with a radius that is a function of the specified linear and angular velocity (Fig. 2.1).

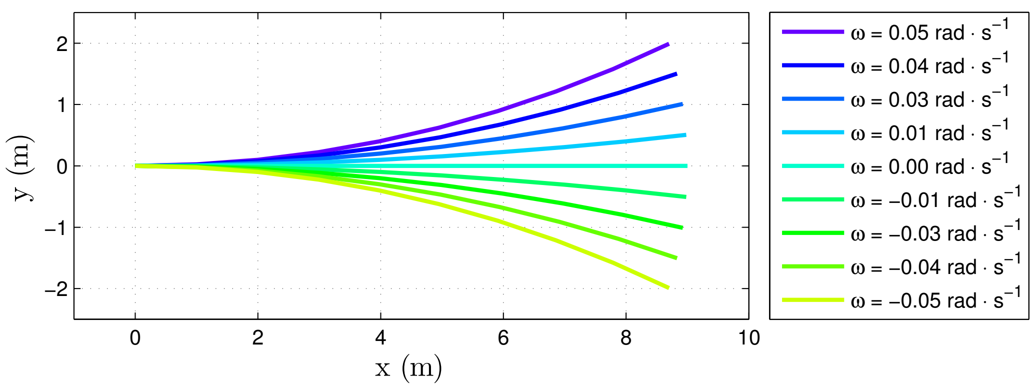

Figure 2.1: Nine motion primitives generated with $\omega = \{-0.05, -0.04, \ldots, 0.05\}$ rad/s, $v = 1.0$ m/s.

Consider a robot following the arc of a circle with velocity v and rotational velocity ω. Assuming the robot's current position is given by $\mathbf{x}_t = (x_t, y_t, \theta_t)^T$, forward-arc motion primitives can be generated by specifying the future robot state, $\mathbf{x}_{t+T}$, as a function of v and ω for a sequence of uniformly varying times $T \in \mathbb{R}^+$. These paths are described by a set of nonlinear differential equations:

$$\dot{\mathbf{x}}_{t+T} = \begin{bmatrix} \dot{x} \\ \dot{y} \\ \dot{\theta} \end{bmatrix}_{t+T} = \begin{bmatrix} v\cos(\theta_{t+T}) \\ v\sin(\theta_{t+T}) \\ \omega \end{bmatrix}, \tag{2.5}$$

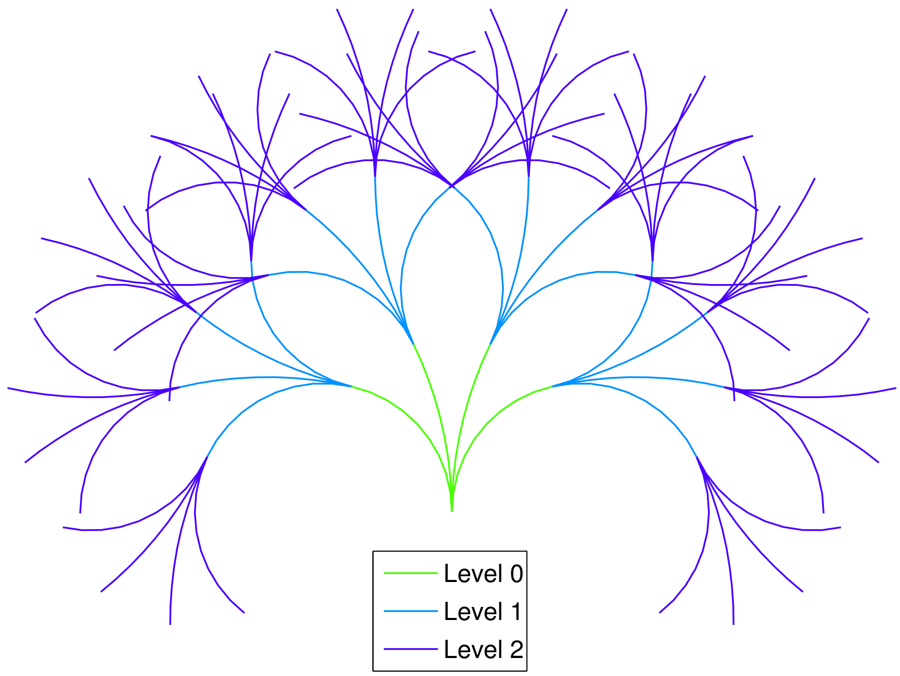

Figure 2.2: A primitive dictionary with a depth of three constructed from a library of four motion primitives.

the solution of which is given by

$$\mathbf{x}_{t+T} = \begin{bmatrix} \frac{v}{\omega}\left(\sin\left(\omega T + \theta_t\right) - \sin\left(\theta_t\right)\right) \\ \frac{v}{\omega}\left(\cos\left(\theta_t\right) - \cos\left(\omega T + \theta_t\right)\right) \\ \omega T \end{bmatrix} + \mathbf{x}_t. \tag{2.6}$$

Sequentially incrementing T in (2.6) produces a sampling of poses lying along an arc parameterized by the robot's velocity and angular velocity, with origin $\mathbf{x}_t$.

A sampling of actions with varying v and w values (such as that depicted in Fig. 2.1) is referred to as a primitive *dictionary*. To generate more actions, one can construct a primitive *library*. This is accomplished by forming a tree with nodes corresponding to poses at the endpoints of actions. The tree is initialized by adding the robot's current position as the root node. Then, a dictionary of motion primitives is rotated and translated to leaf nodes in the tree until a specified depth is reached. A primitive library is shown in Fig. 2.2.

Forward-arc motion primitives are pre-computed prior to deployment into an unknown environment, making them an efficient choice for real-time exploration. Collision checking involves stepping along actions during a breadth-first or depth-first search and pruning all nodes (actions) that lie below those that contain a collision.

2.3.3 Lattice Graph Motion Primitives

A third method for generating actions is lattice graph planning. Lattice graph planners define a discrete set of goal states, and solve Boundary Value Problems (BVPs) to find trajectories from $(\emptyset)$ to each goal [25–27] (Fig. 2.3). The resulting set of motion primitives can be rotated and translated to the robot's current position at run-time, and sampled from to produce candidate actions. Like forward-arc motion primitives, lattice graph motion primitives can be pre-computed and are therefore a suitable choice for real-time exploration. Collision checking for motion primitives in the lattice graph involves stepping along the action and checking for poses that lie outside of the robot's configuration space.

2.4 Generalized Entropies and Divergences

Two fundamental building blocks of information theory are entropy and divergence. The former describes the amount of uncertainty in a random variable, or equivalently, the random variable's information content. The latter is a distance metric between probability distributions that describes the information lost when one distribution is used to describe another. The most well-known forms of entropy and divergence are the Shannon entropy [32], and Kullback-Leibler divergence [21]. For a random variable X, the Shannon entropy, H, and Kullback-Leibler divergence, D_{KL}, are given

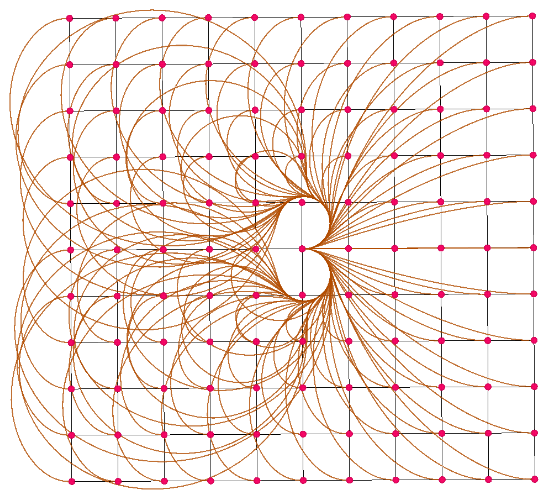

Figure 2.3: An $11 \times 11 \times 1$ lattice graph generated by solving a BVP from the robot's initial pose (middle, facing right) to a lattice of final poses (with final angle equal to initial angle) subject to linear and angular velocity constraints. No solution exists for the nodes immediately above and below the robot's initial position.

by

$$
\begin{aligned}
\mathrm{H}\left(X\right) &= -\sum_{x_i \in \mathcal{X}} P(x_i) \log_2 P(x_i), \\
\mathrm{D}_{\mathrm{KL}}\left(P||Q\right) &= \sum_{x_i \in \mathcal{X}} P(x_i) \log_2 \frac{P(x_i)}{Q(x_i)},
\end{aligned}
\tag{2.7}
$$

where $\mathcal{X}$ is the sample space of X, and P and Q are discrete probability distributions over X. While Shannon entropy and Kullback-Leibler divergence succinctly describe critical concepts of information theory, alternative definitions of these concepts exist.

Shannon entropy is one solution to a more general parametric family of entropies introduced by Rényi [30] that take the (discrete) form

$$
\begin{aligned}
\mathrm{H}_\alpha\left(X\right) &= \frac{1}{1-\alpha} \log_2 \sum_{x_i \in \mathcal{X}} P^\alpha\left(x_i\right) \quad \text{(discrete)} \\
\mathrm{H}_\alpha\left(X\right) &= \frac{1}{1-\alpha} \log_2 \int_{\mathcal{X}} p^\alpha\left(x\right) \quad \text{(continuous)}.
\end{aligned}
\tag{2.8}
$$

Rényi's so-called α-*entropy* approaches the Shannon entropy as $\alpha \to 1^+$, but allows one to express the information content of a random variable using any choice from a family of functions. In some cases H_∞ entropy or H_2 entropy, for example, may be easier to evaluate than Shannon entropy, and carry a similar meaning. Rényi's α-entropy will be used for an optimization that is difficult to solve using Shannon's entropy in Chapter 3.

In a similar nature, there exists a spectrum of divergence measures that generalize and extend the properties of the Kullback-Leibler divergence. The Cauchy-Schwarz (CS) divergence is one measure that is of particular importance to this thesis. CS divergence can be derived by substituting two distributions, P and Q into the Cauchy-

Schwarz inequality [31]:

$$\begin{aligned}
&\sqrt{\sum_{x_i\in\mathcal{X}} P^2(x_i) \sum_{x_i\in\mathcal{X}} Q^2(x_i)} \geq \sum_{x_i\in\mathcal{X}} P(x_i)Q(x_i) \quad \text{(discrete)}\\
&\sqrt{\int_{\mathcal{X}} p^2(x)dx \int_{\mathcal{X}} q^2(x)dx} \geq \int_{\mathcal{X}} p(x)q(x)dx \quad \text{(continuous)}.
\end{aligned} \tag{2.9}$$

CS divergence measures the extent of the inequality in (2.9):

$$\begin{aligned}
\mathrm{D_{CS}}\left(P||Q\right) &= \log \frac{\sum\limits_{x_i\in\mathcal{X}} P^2(x_i) \sum\limits_{x_i\in\mathcal{X}} Q^2(x_i)}{\left(\sum\limits_{x_i\in\mathcal{X}} P(x_i)Q(x_i)\right)^2} \quad \text{(discrete)}\\
\mathrm{D_{CS}}\left(p||q\right) &= \log \frac{\int_{\mathcal{X}} p^2(x)dx \int_{\mathcal{X}} q^2(x)dx}{\left(\int_{\mathcal{X}} p(x)q(x)dx\right)^2} \quad \text{(continuous)}.
\end{aligned} \tag{2.10}$$

CS divergence is a non-negative distance metric that takes on a value of zero when its arguments are the same distribution. Unlike Kullback-Leibler divergence, CS divergence is symmetric in its arguments. It can equivalently be written in terms of Rényi's α-entropy for $\alpha = 2$.

$$\begin{aligned}
\mathrm{D_{CS}}\left(p(x)||q(y)\right) &= -2\log\int_{\mathcal{X},\mathcal{Y}} p(x)q(y)dxdy + \log\int_{\mathcal{X}} p^2(x)dx + \log\int_{\mathcal{Y}} q^2(y)dy\\
&= 2\mathrm{H}_2\left(X;Y\right) - \mathrm{H}_2\left(X\right) - \mathrm{H}_2\left(Y\right),
\end{aligned} \tag{2.11}$$

where $\mathrm{H}_2\left(X;Y\right)$ is the quadratic Rényi cross-entropy [29]:

$$\begin{aligned}
\mathrm{H}_2\left(X;Y\right) &= -\log_2 \sum_{x_i\in\mathcal{X},y_i\in\mathcal{Y}} P(x_i)Q(y_i) \quad \text{(discrete)}\\
\mathrm{H}_2\left(X;Y\right) &= -\log_2 \int p(x)q(y)dxdy \quad \text{(continuous)}.
\end{aligned} \tag{2.12}$$

2.5 Cauchy-Schwarz Quadratic Mutual Information

The CS divergence metric described in Section 2.4 can be used to define a second distance metric that measures the amount of dependence between two random variables X and Y. The amount of dependence between two random variables is synonymous with the definition of mutual information, another fundamental building block of information theory. Mutual information metrics describe the difference between a joint distribution, $p(x, y)$, and the product of its marginals, $p(x)p(y)$. Like entropy and divergence, there exists a common definition for mutual information (the *Shannon mutual information* (SMI)) that can be extended and generalized. In the context of mobile robotic exploration, a more convenient definition of mutual information is the *Cauchy-Schwarz Quadratic mutual information* (CSQMI), which is derived by substituting $p(x, y)$ for p and $p(x)p(y)$ for q in (3.3).

$$\mathrm{I}_{\mathrm{CS}}(X;Y) = \log \frac{\int_{\mathcal{X}} \int_{\mathcal{Y}} p^2(x,y)dxdy \int_{\mathcal{X}} \int_{\mathcal{Y}} p^2(x)p^2(y)dxdy}{\left(\int_{\mathcal{X}} \int_{\mathcal{Y}} p(x,y)p(x)p(y)dxdy\right)^2}. \tag{2.13}$$

Charrow et al. originally showed that the CSQMI between a robot's map and a beam-based sensor measurement is a superior reward metric to SMI for exploration [9]. This is because CSQMI can be computed analytically without requiring an expensive sampling step to calculate the expected value of a future sensor measurement. Additionally, CSQMI can be computed exactly in $\mathcal{O}(n^2)$, and to a close approximation in $\mathcal{O}(n)$, where n is the number of cells in the robot's map intersected by a sequence of beam-based sensor measurements z_τ. While SMI can also be approximated in time linear in n, Charrow et al. show that CSQMI has a smaller linear constant factor, allowing CSQMI to be computed in roughly one seventh of the amount of time. Like

SMI, CSQMI is non-negative and zero only when its arguments are independent (i.e. when $p(x,y) = p(x)p(y)$). Figure 1.4 shows that CSQMI and SMI are similar when evaluated on an OG with a beam-based sensor model, and control actions that maximize CSQMI guide the robot to unexplored space. For discussion regarding explicit calculation of CSQMI, the reader should refer to Charrow et al. [9].

$\mathrm{I}_{\mathrm{CS}}\left(\mathbf{m}; \mathbf{z}_\tau\left(\mathbf{x}_\tau\right)\right)$ is therefore a suitable choice for $\mathcal{J}\left(\mathbf{m}; \mathbf{z}_\tau\left(\mathbf{x}_\tau\right)\right)$ in (2.4). The map $\mathbf{m}$ is considered to be a discrete multivariate random variable because its sample space is discrete (cells may only be `OCC` or `EMP`), so CSQMI between an OG map and sequence of beam-based measurements is

$$\mathrm{I}_{\mathrm{CS}}\left(\mathbf{m}; \mathbf{z}_\tau\right) = \log \frac{\int \sum_{\mathcal{M}} p^2(\mathbf{m}, \mathbf{z}_\tau) d\mathbf{z}_\tau \int \sum_{M} p^2(\mathbf{m}) p^2(\mathbf{z}_\tau) d\mathbf{z}_\tau}{\left(\int \sum_{\mathcal{M}} p(\mathbf{m}) p(\mathbf{z}_\tau) p(\mathbf{m}, \mathbf{z}_\tau) d\mathbf{z}_\tau\right)^2}, \tag{2.14}$$

where $\mathcal{M}$ is a set of all possible map permutations. Substituting I_{CS} for $\mathcal{J}$ in (2.4) yields an active perception optimization that guides a robot towards unexplored locations in its map by maximizing an information-theoretic reward functional.

$$\mathbf{x}_\tau^* = \underset{\mathbf{x}_\tau \in \mathcal{X}}{\operatorname{argmax}} \; \mathrm{I}_{\mathrm{CS}}\left(\mathbf{m}, \mathbf{z}_\tau(\mathbf{x}_\tau)\right). \tag{2.15}$$

2.6 Summary of Foundations

Chapter 2 reviewed foundational elements that will be used for derivations in the remaining chapters. These elements culminate in an optimization that drives a robot towards unexplored space in its map by maximizing an information-theoretic reward function (2.15). The chosen reward function, CSQMI [28], resembles Shannon's original definition of mutual information, but can be computed more efficiently when its arguments are an OG map and a sequence time-ordered beam-based sensor measurements [9].

Furthermore, Chapter 2 discussed three methods for generating dynamically feasible and collision-free actions through the robot's configuration space. The action maximizing CSQMI (either integrated over the path, or at the action's final pose) will be chosen as that which optimally drives the robot towards unexplored space. The remainder of this thesis will use both forward-arc motion primitives and lattice graph motion primitives for action generation, although the third option - frontier seeding - is equally viable.

Chapter 3

Information-Theoretic Map Compression

The remaining chapters of this thesis introduce novel extensions to active perception that make information-theoretic reward evaluation orders of magnitude more efficient at the cost of information accuracy (Chapter 4), and allow the robot to implicitly consider and avoid complex regions in its local map while simultaneously planning informative paths (Chapter 5). Both of these extensions originate from the observation that the information content of a robot's sensor measurement depends on the environment representation. In the case of OG maps, the cell resolution parameter shares an intricate relationship with the robot's exploration behaviors.

One example of the relationship between OG cell resolution and exploration behavior lies in the efficiency of raycasting. Most information-theoretic reward functions (e.g. SMI and CSQMI) require simulating a beam-based sensor measurement from a future position, which implicitly requires raycasting through the map. Intuitively, as the resolution of cells in the map decreases, so too does the number of cells that a raycast must traverse. Therefore the efficiency of information-theoretic reward evalu-

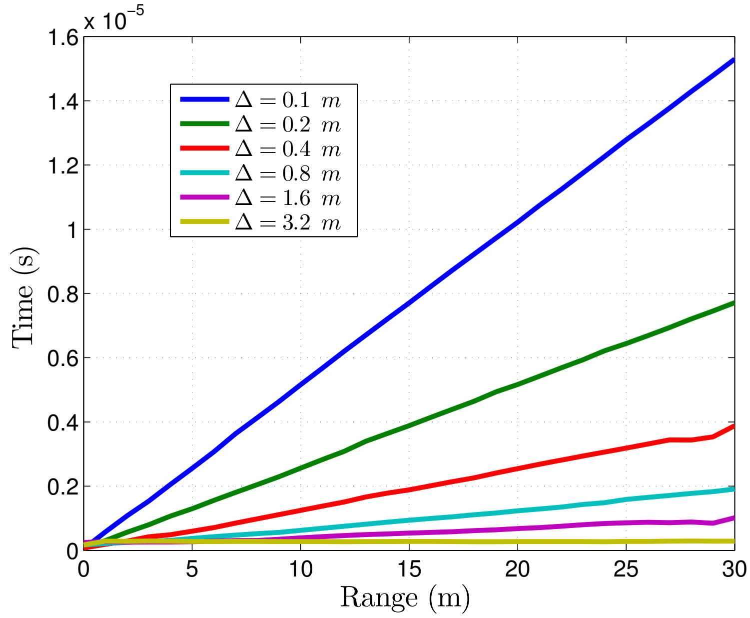

Figure 3.1: Time (median of 10^5 samples) to evaluate CSQMI for a single beam is linear in both the OG resolution Δ, and the measurement range.

ation is a function of the cell resolution of the OG. For example, using the approximate CSQMI technique from Charrow et al. [9], this relationship is linear (Fig. 3.1). As will be shown, the resolution of an OG map can typically be halved several times before a significant amount of information about free and occupied space is lost. However, sequentially halving the resolution exponentially increases the speed of computing CSQMI, regardless of sensor range or number of beams. This can be seen by holding range constant and tracing vertical lines down Fig. 3.1.

The incentive for increasing the efficiency of information-theoretic exploration is clear and immediate; any reduction to the time required to evaluate an information-theoretic reward function will enable robots to explore at higher speeds, in turn allowing them to initialize (build a map) faster, or clear a building for threats more quickly. However, at present, there is no clear choice of algorithm for compressing an OG from one resolution to another.

Several others have proposed strategies for map compression. The OctoMap framework [39] builds an octree data structure to efficiently store the expected occupancy of cells in an environment without allocating memory for a large 3D grid. Jeong et al. [15] compress an OG be representing it with wavelets using the Haar wavelet transform. Kretzschmar et al. [20] compress pose graph maps by examining the Shannon mutual information between the pose graph and sensor measurements. Most related to the problem framed here is the work by Einhorn et al. [10], which adaptively chooses an OG resolution for individual cells by determining which cells are intersected by measurements.

Instead, the following chapter describes the first main contribution of this thesis: a novel strategy for OG compression using the Principle of Relevant Information [28]. In contrast to previous works on map compression, this strategy approaches the compression problem from an information theory perspective, optimizing a functional that describes the distortion between the map and its compressed form. The proposed map compression strategy yields an exceedingly simple compression algorithm that is founded on rate distortion theory. This compression algorithm acts as a basis for the active perception extensions introduced in Chapters 4 and 5.

3.1 The Principle of Relevant Information

The OG compression problem can be formulated as an information-theoretic optimization using the Principle of Relevant Information (PRI). PRI is a technique for learning a reduced representation $\hat{X}$ of a random variable X such that both the entropy of $\hat{X}$ and the divergence of $\hat{X}$ with respect to the original data are minimized.

$$J(\hat{X}) = \min_{\hat{X}}(\mathrm{H}_\alpha(\hat{X}) + \lambda \mathrm{D}_\alpha(X||\hat{X})). \tag{3.1}$$

The two terms of the PRI cost function are Rényi's α-entropy, which describes the amount of uncertainty in its argument, and Rényi's α-divergence, which is a distance measure describing distortion between $p(x)$ and $p(\hat{x})$. These terms simplify to the more common Shannon entropy and Kullback-Leibler divergence for $\alpha = 1$. The variational parameter λ controls the amount of distortion in the compressed data. Following Principe et al., we choose to minimize the H_2 entropy and Cauchy-Schwarz divergence. For discrete random variables X and $\hat{X}$,

$$\mathrm{H}_2(\hat{X}) = -\log \sum_i p^2(\hat{x}_i), \tag{3.2}$$

$$\mathrm{D}_{\mathrm{CS}}(X||\hat{X}) = \log \frac{\sum_i p^2(x_i) \sum_i p^2(\hat{x}_i)}{\left(\sum_i p(x_i)p(\hat{x}_i)\right)^2}. \tag{3.3}$$

The cost function in (3.1) is then:

$$(1-\lambda)\,\mathrm{H}_2(\hat{X}) - \lambda 2 \log \sum_i p(x_i)p(\hat{x}_i) - \lambda \mathrm{H}_2(X). \tag{3.4}$$

The third term has no influence on the minimization over $\hat{X}$, and can be ignored. We choose to give equal weight to the entropy and divergence, and optimize for $\lambda = 1$. Noting that logs and quadratic functions increase monotonically for positive arguments, and noting that the summand in the second term of (3.4) must be positive, the optimization can be simplified to:

$$J(\hat{X}) = \max_{\hat{X}} \sum_i p(x_i)p(\hat{x}_i). \tag{3.5}$$

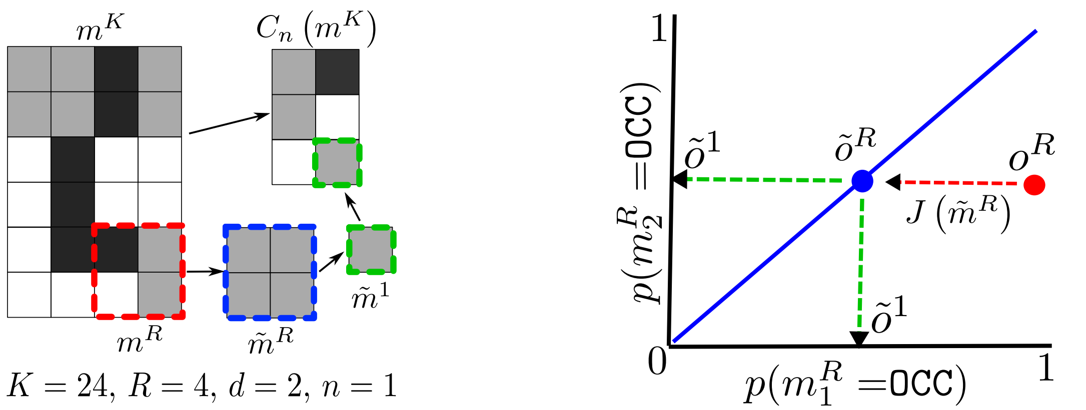

(a) OG compression sequence

(b) Probability space of the top two grid cells in m^R in 3.2a

Figure 3.2: For each square (cubic in 3D) region m^R in the uncompressed OG m^K, the PRI optimization finds a random variable $\tilde{m}^R$ that minimizes (3.1) and is constrained to have uniform occupancy probability $\tilde{o}^R = (\tilde{o}^1, \ldots, \tilde{o}^1)$.

3.2 Framing Map Compression as an Optimization

To apply the PRI optimization to OG compression, let X be an OG m^K with K cells. The problem must be constrained in three ways. First, because OGs encode a 2D or 3D geometry, $\hat{X}$ must represent X well in local regions. Compression over the map can therefore be accomplished by performing compression in many small independent square (cubic in 3D) regions $m^R \subseteq m^K$, assuming individual grid cell occupancies are independent. Second, we consider only the set of compressions that reduce OG cell count in each dimension by factors of two. Therefore an OG m^K will be compressed to an OG $m^{2^{-dn}K}$, where d is the OG dimension and n is the number of $2\times$ compressions in each dimension. The set of compressions with this property can be expressed as:

$$C_n(m^K) \equiv m^{2^{-dn}K}, \quad n \in \mathbb{N}_0, \tag{3.6}$$

where superscripts denote cell count and where a compression of $n = 0$ gives the original OG: $C_0(m^K) = m^K$. Both m^K and $C_n(m^K)$ will have the same metric dimensions, but will have different cell edge lengths and cell counts when $n \geq 1$. Finally, we enforce that $\hat{X}$ must also be an OG. Since $\mathrm{D_{CS}}(X||\hat{X})$ may only be computed for two random variables with the same support set, we use the PRI to find a random variable $\tilde{m}^R$ that has uniform occupancy probabilities, and then reduce its dimension to one, yielding a single grid cell $\tilde{m}^1$ (Fig. 3.2). Combining the single-cell $\tilde{m}^1$ variables from independent regions yields the compressed OG $C_n(m^K)$.

Rather than directly maximizing (3.5) over $\tilde{m}^R$, we are interested in finding the distribution $p(\tilde{m}^R)$ corresponding to the maximum. $p(\tilde{m}^R)$ is a Bernoulli distribution, and is completely determined by its single parameter $\tilde{o}^1 = p(\tilde{m}^R = \{\texttt{OCC}, \ldots, \texttt{OCC}\}) =$

$1 - p(\tilde{m}^R = \{\texttt{EMP}, \ldots, \texttt{EMP}\})$. Substituting the described variables into (3.5),

$$\tilde{o}^1_* = \underset{\tilde{o}^1}{\text{argmax}} \sum_{M^R} p\left(m^R = M^R\right) p\left(\tilde{m}^R = M^R\right). \tag{3.7}$$

3.3 Solving the Optimization

Table 3.1 shows a contingency table for a compression from the OG region m^R to $\tilde{m}^R$. The middle columns of the contingency table have zero probability, since the $\tilde{m}^R$ must have a uniform cell probability to be able to reduce it to $\tilde{m}^1$ (i.e. $\tilde{o}^R_i = \tilde{o}^R_j = \tilde{o}^1 \, \forall i, j \in 1, \ldots, R$). In this section we are only interested in the marginal distributions (bottom-most row and right-most column), which are needed to determine (3.7). Substituting these,

$$\tilde{o}^1_* = = \underset{\tilde{o}^1}{\text{argmax}} \left((1 - \tilde{o}^1) \prod_{i=1}^{R} (1 - o^R_i) + \tilde{o}^1 \prod_{i=1}^{R} o^R_i \right), \tag{3.8}$$

which is satisfied for

$$\tilde{o}^1_* = \begin{cases} 0 & \text{if } \prod_{i=1}^{R} \frac{o^R_i}{1 - o^R_i} < 1 \\ 1 & \text{if } \prod_{i=1}^{R} \frac{o^R_i}{1 - o^R_i} > 1 \\ \frac{1}{2} & \text{otherwise} \end{cases}, \tag{3.9}$$

where the last case applies in the limit as $\lambda \to 1^+$.

The PRI solution gives us a simple compression rule: if the product of cell occupancy likelihoods in a given region is greater than 1, set the occupancy of the cell corresponding to that region in the compressed OG to 1. Likewise set the value to 0 if the product of likelihoods is less than 1, and to 0.5 if the product of likelihoods is

1. Pragmatically, it is more reasonable to use the map's occupancy and free thresholds rather than 1.0 and 0.0. This variation corresponds to optimizing for λ slightly greater than one, favoring minimal distortion to minimal entropy. Additionally, one may introduce a heuristic to increase the fraction of occupied cells that are preserved through compression by multiplying the right-hand sides of the inequalities in (3.9) by $\eta \in (0, 1)$. As η decreases, occupied cells will be preserved through compression with higher frequency. For any application involving raycasting, it is especially important to include this heuristic, as vanishing occupied cells lead to poor ray termination.

Denoting $\pi^R \equiv \prod_{i=1}^{R} \frac{o_i^R}{1-o_i^R}$ and applying these modifications gives the $\sqrt{R} \times \sqrt{R} \rightarrow 1 \times 1$ (or $\sqrt[3]{R} \times \sqrt[3]{R} \times \sqrt[3]{R} \rightarrow 1 \times 1 \times 1$ in 3D) compression rule for each region m^R:

$$\tilde{o}_*^1 = \begin{cases} \frac{1}{2} & \text{if } \pi^R = \eta \vee \pi^R = 1 \\ p_{\text{free}} & \text{if } \pi^R < \eta \wedge \pi^R \neq 1 \\ p_{\text{occ}} & \text{if } \pi^R > \eta \wedge \pi^R \neq 1 \end{cases}, \tag{3.10}$$

where p_{occ} and p_{free} are the thresholds for occupied and free space in the OG implementation, respectively.

3.4 Occupancy Grid Pyramids

3.5 Results

3.6 Chapter Summary

Table 3.1: Contingency table for a compression from the OG region m^R to $\tilde{m}^R$. `O` and `E` stand for `OCC` and `EMP`.

		$\tilde{m}^R$					
		`E, E, ..., E`	`E, E, ..., O`	$\dots$	`O, O, ..., E`	`O, O, ..., O`	Total
m^R	`E, E, ..., E`	$w_2 \cdot (1-\tilde{o}^1) \cdot \prod_{i=1}^R (1-o_i^R)$	0	$\dots$	0	$w_3 \cdot \tilde{o}^1 \cdot \prod_{i=1}^R (1-o_i^R)$	$\prod_{i=1}^R (1-o_i^R)$
	`E, E, ..., O`	$w_1 \cdot (1-\tilde{o}^1) \cdot o_1^R \cdot \prod_{i=2}^R (1-o_i^R)$	0	$\dots$	0	$w_4 \cdot \tilde{o}^1 \cdot o_1 \cdot \prod_{i=2}^R (1-o_i^R)$	$o_1 \cdot \prod_{i=2}^R (1-o_i^R)$
	$\vdots$	$\vdots$	$\vdots$	$\ddots$	$\vdots$	$\vdots$	$\vdots$
	`O, O, ..., E`	$w_1 \cdot (1-\tilde{o}^1) \cdot (1-o_1^R) \cdot \prod_{i=2}^R o_i^R$	0	$\dots$	0	$w_4 \cdot \tilde{o}^1 \cdot (1-o_1^R) \cdot \prod_{i=2}^R o_i^R$	$(1-o_1^R) \cdot \prod_{i=2}^R o_i^R$
	`O, O, ..., O`	$w_1 \cdot (1-\tilde{o}^1) \cdot \prod_{i=1}^R o_i^R$	0	$\dots$	0	$w_4 \cdot \tilde{o}^1 \cdot \prod_{i=1}^R o_i^R$	$\prod_{i=1}^R o_i^R$
	Total	$1-\tilde{o}^1$	0	$\dots$	0	$\tilde{o}^1$	1

Chapter 4

The PRI strategy in Sec. **??** determines an optimal compression given a desired OG resolution. However, Fig. 3.1 suggests that one should also reduce the resolution of the OG as much as possible to increase efficiency. In this section we formulate a second optimization based on the Information Bottleneck (IB) method [**?**] that chooses a grid resolution minimizing both the redundancy between m^K and $C_n(m^K)$, and loss of mutual information with respect to a sensor measurement z.

4.1 The Information Bottleneck Method

IB is a widely used technique in signal processing for finding the optimal reduced representation $\hat{X}$ of a random variable X that preserves maximum information about a second random variable Y:

$$\min_{\hat{X}} \mathrm{I}(X; \hat{X}) - \beta \mathrm{I}(\hat{X}; Y). \tag{4.1}$$

IB resembles PRI, but considers the effects of compression on the information between two datasets, as opposed to one. Similar to λ in the PRI optimization, β is a design parameter that trades compression for conservation of information. As $\beta \to 0$, the optimization tends towards the trivial lossy compression $\{\hat{X}\} = 0$, whereas when

$\beta \to \infty$, $\hat{X}$ approaches its original representation X [28]. The two terms in the argument of (4.1) can equivalently be thought of as the information loss incurred by describing $\hat{X}$ with Y instead of with X [?].

Most importantly for OG compression, when combined with the PRI approach in Section ??, the IB method can be used to find an optimal compression n^*:

$$n^* = \underset{n \in \mathbb{N}_0}{\operatorname{argmin}} \; \mathrm{I}_{\mathrm{CS}}\left(m^K; C_n(m^K)\right) - \beta \mathrm{I}_{\mathrm{CS}}\left(C_n(m^K); z\right). \tag{4.2}$$

4.2 Optimizing Map Resolution for Sensing

The second term can be computed using (??), and is $2^{1 \times n}$ times more efficient than computing (??) with respect to the uncompressed map m^K (where $d = 1$ because $\mathrm{I}_{\mathrm{CS}}(m; z_\tau)$ is computed using 1D raycasts). Since $\mathrm{I}_{\mathrm{CS}}(m^K; C_n(m^K))$ describes the divergence between the distributions $p(m^K, C_n(m^K))$ and $p(m^K)p(C_n(m^K))$, the first term in (??) can be computed by substituting these for $p(x_i)$ and $p(\hat{x}_i)$ in the definition of Cauchy-Schwarz divergence (3.3).

However, the joint distribution $p(m^K, C_n(m^K))$ is underdetermined by two variables, and must be constrained before computing (4.2). While the remaining two degrees of freedom make the IB cost function arbitrary for a single resolution, fixing the joint distribution and using it to compute CSQMI across different grid resolutions still yields a meaningful optimization. To constrain the extra degrees of freedom we first decompose the joint distribution into independent regions $r \in m^K$:

$$\begin{aligned} p(m^K, C_n(m^K)) &= \prod_{r \in m^K} p(m_r^R, C_n(m_r^R)) \\ &= \prod_{r \in m^K} p(m_r^R, \tilde{m}_r^R), \end{aligned} \tag{4.3}$$

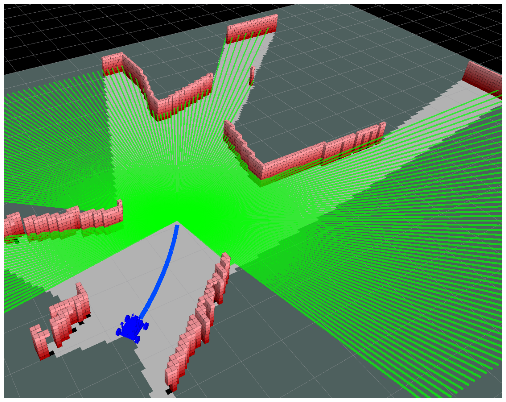

(a)

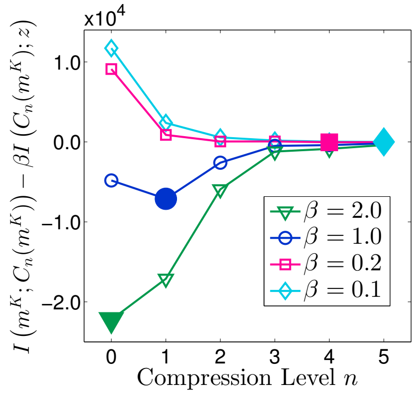

(b)

Figure 4.1: 4.1a shows an uncompressed map and measurement taken from a planned future position. With this map and expected laser scan, the optimal compression level (filled markers) computed with (4.2) decreases as β increases, favoring preservation of information about the measurement as opposed to compression (4.1b).

where the second equation holds by noting $C_n(m_r^R)$ has a dimension of one, and that that all cells in $\tilde{m}^r$ are completely determined by knowing $C_n(m_r^R)$. Then, for each region r, we choose the joint distribution $p(m_r^R, \tilde{m}_r^R))$ to be a product of the marginals $p(m_r^R)$ and $p(\tilde{m}_r^R))$, weighted by four extra coefficients $w_{1:4}$ (Table 3.1). Similar to the reasons that η in Sec. **??** is chosen to preserve occupied cells through compression, the constant $c_1 \in (0, 1)$ downweighs the probability of the event that $\tilde{m}^R$ is $\{\texttt{EMP}, \ldots, \texttt{EMP}\}$ if any grid cells in m^R are occupied. The remaining three constants balance the effects of w_1 such that the conditional distributions over the rows and columns of Table 3.1 all sum to the marginal distributions on the bottom-most row and right-most column.

Figure 4.1 displays the influence of β on the IB optimization for a multi-beam measurement captured from a planned future location. The optimization favors no compression when β is large, and maximum compression when β is small.

4.3 Results

4.4 Chapter Summary

Chapter 5

Additionally, the information lost when compressing an OG map from one cell resolution to another correlates with the *complexity* of the map - the density of free and occupied space.

5.1 Results

5.2 Chapter Summary

Chapter 6

Summary, Contributions, and Future Work

6.1 Thesis Summary

6.2 Contributions

6.3 Future Work

6.4 Conclusions

Bibliography

[1] Ercan U Acar and Howie Choset. Sensor-based coverage of unknown environments: Incremental construction of morse decompositions. *The International Journal of Robotics Research*, 21(4):345–366, 2002.

[2] Francesco Amigoni and Vincenzo Caglioti. An information-based exploration strategy for environment mapping with mobile robots. *Robotics and Autonomous Systems*, 58(5):684–699, 2010.

[3] Ruzena Bajcsy. Active perception. *Proceedings of the IEEE*, 76(8):966–1005, 1988.

[4] Ruzena Bajcsy and Mario Campos. Active and exploratory perception. *CVGIP: Image Understanding*, 56(1):31–40, 1992.

[5] Nicola Basilico and Francesco Amigoni. On evaluating performance of exploration strategies for autonomous mobile robots. In *Proceedings of the performance evaluation and benchmarking for intelligent robots and systems workshop at IEEE/RSJ international conference on intelligent robots and systems*, 2008.

[6] Frederic Bourgault, Alexei A Makarenko, Stefan B Williams, Ben Grocholsky, and Hugh F Durrant-Whyte. Information based adaptive robotic exploration. In

Intelligent Robots and Systems, 2002. IEEE/RSJ International Conference on, volume 1, pages 540–545. IEEE, 2002.

[7] Wolfram Burgard, Mark Moors, Dieter Fox, Reid Simmons, and Sebastian Thrun. Collaborative multi-robot exploration. In *Robotics and Automation, 2000. Proceedings. ICRA'00. IEEE International Conference on*, volume 1, pages 476–481. IEEE, 2000.

[8] Kwong-Fai Chan and Tak Wah Lam. An on-line algorithm for navigating in an unknown environment. *International Journal of Computational Geometry & Applications*, 3(03):227–244, 1993.

[9] Ben Charrow, Sikang Liu, Vijay Kumar, and Nathan Michael. Information-theoretic mapping using cauchy-schwarz quadratic mutual information. In *Robotics and Automation, 2015. Proceedings., 2015 IEEE International Conference on*. IEEE, 2015.

[10] Erik Einhorn, C Schroter, and H Gross. Finding the adequate resolution for grid mapping-cell sizes locally adapting on-the-fly. In *Robotics and Automation (ICRA), 2011 IEEE International Conference on*, pages 1843–1848. IEEE, 2011.

[11] Hans Jacob S Feder, John J Leonard, and Christopher M Smith. Adaptive mobile robot navigation and mapping. *The International Journal of Robotics Research*, 18(7):650–668, 1999.

[12] Hector H Gonzalez-Banos and Jean-Claude Latombe. Navigation strategies for exploring indoor environments. *The International Journal of Robotics Research*, 21(10-11):829–848, 2002.

[13] Peter E Hart, Nils J Nilsson, and Bertram Raphael. A formal basis for the heuristic determination of minimum cost paths. *Systems Science and Cybernetics, IEEE Transactions on*, 4(2):100–107, 1968.

[14] Dirk Holz, Nicola Basilico, Francesco Amigoni, and Sven Behnke. A comparative evaluation of exploration strategies and heuristics to improve them. In *ECMR*, pages 25–30, 2011.

[15] Jeong Joon Im, Alexander Leonessa, and Andrew Kurdila. A real-time data compression and occupancy grid map generation for ground-based 3d lidar data using wavelets. In *3rd ASME Dynamic Systems and Control Conference, Boston, MA*, 2010.

[16] Brian J Julian, Sertac Karaman, and Daniela Rus. On mutual information-based control of range sensing robots for mapping applications. In *Intelligent Robots and Systems (IROS), 2013 IEEE/RSJ International Conference on*, pages 5156–5163. IEEE, 2013.

[17] Brian John Julian. *Mutual information-based gradient-ascent control for distributed robotics*. PhD thesis, Massachusetts Institute of Technology, 2013.

[18] Thomas Kollar and Nicholas Roy. Efficient optimization of information-theoretic exploration in slam. In *AAAI*, volume 8, pages 1369–1375, 2008.

[19] Thomas Kollar and Nicholas Roy. Trajectory optimization using reinforcement learning for map exploration. *The International Journal of Robotics Research*, 27(2):175–196, 2008.

[20] Henrik Kretzschmar and Cyrill Stachniss. Information-theoretic compression of pose graphs for laser-based slam. *The International Journal of Robotics Research*, 31(11):1219–1230, 2012.

[21] Solomon Kullback and Richard A Leibler. On information and sufficiency. *The annals of mathematical statistics*, pages 79–86, 1951.

[22] Steven M LaValle. Rapidly-exploring random trees a ew tool for path planning. Technical report, Compute Science Department, Iowa State University, 1998.

[23] Steven M LaValle. *Planning algorithms*. Cambridge university press, 2006.

[24] Erik Nelson and Nathan Michael. Optimal information-theoretic occupancy grid compression for high-speed information-based exploration. In *IEEE/RSJ International Conference on Intelligent Robots and Systems, 2015. (IROS 2015)*. IEEE, 2015.

[25] Mihail Pivtoraiko and Alonzo Kelly. Generating near minimal spanning control sets for constrained motion planning in discrete state spaces. In *Intelligent Robots and Systems, 2005.(IROS 2005). 2005 IEEE/RSJ International Conference on*, pages 3231–3237. IEEE, 2005.

[26] Mihail Pivtoraiko, Ross A Knepper, and Alonzo Kelly. Differentially constrained mobile robot motion planning in state lattices. *Journal of Field Robotics*, 26(3):308–333, 2009.

[27] Mihail Pivtoraiko, Daniel Mellinger, and Vijay Kumar. Incremental micro-uav motion replanning for exploring unknown environments. In *Robotics and Automation (ICRA), 2013 IEEE International Conference on*, pages 2452–2458. IEEE, 2013.

[28] Jose C Principe. *Information theoretic learning: Rényi's entropy and kernel perspectives*. Springer Science & Business Media, 2010.

[29] S Rao. *Unsupervised Learning: An Information Theoretic Learning Approach.* PhD thesis, University of Florida, Gainesville, 2008.

[30] Alfred Renyi. On measures of entropy and information. In *Fourth Berkeley symposium on mathematical statistics and probability*, volume 1, pages 547–561, 1961.

[31] Walter Rudin. *Principles of mathematical analysis*, volume 3. McGraw-Hill New York, 1964.

[32] Claude Elwood Shannon. A mathematical theory of communication. *Bell System Technical Journal*, 27:379–423, 1948.

[33] Shaojie Shen, Nathan Michael, and Vijay Kumar. Autonomous indoor 3d exploration with a micro-aerial vehicle. In *Robotics and Automation (ICRA), 2012 IEEE International Conference on*, pages 9–15. IEEE, 2012.

[34] Robert Sim, Gregory Dudek, and Nicholas Roy. Online control policy optimization for minimizing map uncertainty during exploration. In *Robotics and Autkollar2008trajectoryomation, 2004. Proceedings. ICRA'04. 2004 IEEE International Conference on*, volume 2, pages 1758–1763. IEEE, 2004.

[35] Camillo J Taylor and D Kriegman. Exploration strategies for mobile robots. In *Robotics and Automation, 1993. Proceedings., 1993 IEEE International Conference on*, pages 248–253. IEEE, 1993.

[36] Sebastian Thrun, Wolfram Burgard, and Dieter Fox. *Probabilistic robotics.* MIT press, 2005.

[37] Joan Vallvé and Juan Andrade-Cetto. Dense entropy decrease estimation for mobile robot exploration. In *Robotics and Automation (ICRA), 2014 IEEE International Conference on*, pages 6083–6089. IEEE, 2014.

[38] Pengpeng Wang. *View planning with combined view and travel cost*. PhD thesis, School of Engineering Science-Simon Fraser University, 2007.

[39] Kai M Wurm, Armin Hornung, Maren Bennewitz, Cyrill Stachniss, and Wolfram Burgard. Octomap: A probabilistic, flexible, and compact 3d map representation for robotic systems. In *Proc. of the ICRA 2010 workshop on best practice in 3D perception and modeling for mobile manipulation*, volume 2, 2010.

[40] Brian Yamauchi. A frontier-based approach for autonomous exploration. In *Computational Intelligence in Robotics and Automation, 1997. CIRA'97., Proceedings., 1997 IEEE International Symposium on*, pages 146–151. IEEE, 1997.